Journal of Hazardous Materials 163 (2009) 973–981

Contents lists available at ScienceDirect

Journal of Hazardous Materials

journal homepage: www.elsevier.com/locate/jhazmat

Photocatalytic degradation of *p*-phenylenediamine with TiO_2-coated magnetic PMMA microspheres in an aqueous solution

Yi-Hung Chen[a,*], Yi-You Liu[b], Rong-Hsien Lin[b], Fu-Shan Yen[b]

[a] *Department of Chemical Engineering and Biotechnology, National Taipei University of Technology, 1, Sec. 3, Chung-Hsiao E. Road, Taipei 106, Taiwan*
[b] *Department of Chemical and Material Engineering, National Kaohsiung University of Applied Sciences, 415 Chien Kung Road, Kaohsiung 807, Taiwan*

ARTICLE INFO

Article history:
Received 8 March 2008
Received in revised form 26 June 2008
Accepted 11 July 2008
Available online 30 July 2008

Keywords:
p-Phenylenediamine
Photocatalytic degradation
UV radiation
Titanium dioxide
Magnetic poly(methyl methacrylate)

ABSTRACT

This study investigates the photocatalytic degradation of *p*-phenylenediamine (PPD) with titanium dioxide-coated magnetic poly(methyl methacrylate) (TiO_2/mPMMA) microspheres. The TiO_2/mPMMA microspheres are employed as novel photocatalysts with the advantages of high photocatalytic activity, magnetic separability, and good durability. The scanning electron microscopy (SEM), energy dispersive spectrometer (EDS), and transmission electron microscopy (TEM) images of the TiO_2/mPMMA microspheres are used to characterize the morphology, element content, and distribution patterns of magnetite and TiO_2 nanoparticles. The BET-specific surface area and saturation magnetization of the TiO_2/mPMMA microspheres are observed as 2.21 m^2/g and 4.81 emu/g, respectively. The photocatalytic degradation of PPD are performed under various experimental conditions to examine the effects of initial PPD concentration, TiO_2/mPMMA microsphere dosage, and illumination condition on the eliminations of PPD and chemical oxygen demand (COD) concentrations. Good repeatability of photocatalytic performance with the use of the TiO_2/mPMMA microspheres has been demonstrated in the multi-run experiments. The photocatalytic kinetics for the reductions of PPD and COD associated with the initial PPD concentration, UV radiation intensity, and TiO_2/mPMMA microsphere dosage are proposed. The relationships between the reduction percentages of COD and PPD are clearly presented.

1. Introduction

p-Phenylenediamine (PPD), also named 1,4-diaminobenzene or 1,4-phenylenediamine, is an aromatic amine used as a component of engineering polymers and composites, aramid fibers, hair dyes, rubber chemicals, textile dyes, and pigments. However, PPD has been found to be hazardous in case of ingestion, inhalation, skin contact, and eye contact [1–3]. Acute exposure to high level of PPD concentration may cause severe dermatitis, eye irritation and tearing, asthma, gastritis, renal failure, vertigo, tremors, convulsions, and coma in humans [4,5].

Titanium dioxide (TiO_2) pigment is a fine and white powder that provides for excellent whiteness and opacity in paints, plastics, and paper. These unique properties are derived from the higher refractive index of TiO_2 that expresses the ability to scatter light. TiO_2 is known to be a promising material for a practical photocatalyst in the removal of organic pollutants [6]. However, the commercial TiO_2 photocatalyst usually has a small particle size that is hard to recover after use and tends to cause the accumulation or blocking in the instruments, thus limiting its practical use. Magnetic composites such as magnetic polymer microspheres have created great interest and application in the biotechnology and medicine fields during the past years [7,8]. The magnetic polymer microspheres can be effectively separated and collected in the environment of the magnetic field that is appropriate for application in the areas of the cell isolation, enzyme immobilization, protein and enzyme purification, water treatment, and targeting drug [9–14].

The contribution of the present paper is to further modify the magnetic poly(methyl methacrylate) (mPMMA) microspheres which were synthesized using a modified suspension polymerization [15]. The novel TiO_2-coated magnetic poly(methyl methacrylate) (TiO_2/mPMMA) microspheres is obtained by the modified suspension polymerization and the following titania-coating process in this study. The magnetic polymer microspheres have a particle diameter of several micrometers, a narrow size distribution, and high magnetite content. The magnetic polymer microspheres with nonporous structure are favorable for further surface modification and can be applied as ideal magnetic car-

* Corresponding author. Tel.: +886 932 234945.
E-mail address: yhchen1@ntu.edu.tw (Y.-H. Chen).

0304-3894/$ – see front matter © 2008 Elsevier B.V. All rights reserved.
doi:10.1016/j.jhazmat.2008.07.097

Nomenclature

A_q	outer area of quartz tubes submerged in solution (cm^2)
C_{BLb}	concentration of PPD in solution (mg/L)
C_{BLb0}	initial concentration of PPD in solution (mg/L)
C_{COD}	concentration of COD in solution (mg/L)
C_{COD0}	initial concentration of COD in solution (mg/L)
COD	chemical oxidation demand
F_s	fraction of emitting light absorbed by solution
Hc	coercivity (Oe)
$[I]$	UV radiation intensity (W/L)
$[I_{254}]$	UV radiation intensity at 254 nm (W/L)
$[I_{365}]$	UV radiation intensity at 365 nm (W/L)
$[I_{UV}]$	light intensity measured on outer surface of quartz tubes (W/cm^2)
k_B	photocatalytic reaction rate constant in Eq. (1) (mg/(L min))
k_B'	modified k_B in Eq. (2), $k_B' = k_B/[I_{254}]$ (mg/(W min))
k_{COD}	photocatalytic oxidation rate constant in Eq. (3) (min^{-1})
K_B	equilibrium adsorption constant of Langmuir's isotherm in Eq. (1) (L/mg)
K_{ow}	octanol/water partition coefficient
mPMMA	magnetic poly(methyl methacrylate)
Mr	residual magnetization per gram (emu/g)
Ms	saturation magnetization per gram (emu/g)
OMP	oleic acid-coated magnetite nanoparticles
PPD	*p*-phenylenediamine
r_0	initial photocatalytic reaction rate (mg/(L min))
R^2	determination coefficient
t	time (min)
TiO_2	titanium dioxide
TiO_2/mPMMA	titanium dioxide-coated magnetic poly(methyl methacrylate)
UV	ultraviolet
V_L	volume of solution (L)
W_{cat}	TiO_2/mPMMA microsphere dosage (g/L)

Greek letters

η_{BLb}	reduction percentage of PPD (%), $=1 - C_{BLb}/C_{BLb0}$
η_{COD}	reduction percentage of COD (%), $=1 - C_{COD}/C_{COD0}$
θ_B	initial fraction of TiO_2 surface covered by PPD, $=K_B C_{BLb0}/(1 + K_B C_{BLb0})$

riers. Commercial TiO_2 nanoparticles (Degussa P-25) are directly employed in the coating process to reduce the synthetic complexity and cost.

Furthermore, this study is to investigate the photocatalytic degradation of PPD with the TiO_2/mPMMA microspheres in an aqueous solution. The available information about the photocatalytic degradation of PPD is found scarce and desirable. As a result, the good magnetic and photocatalytic characteristics of the TiO_2/mPMMA microspheres are presented from their abundant magnetite and photocatalyst contents. Thus the TiO_2/mPMMA microspheres have high potential to be applied in both the slurry photocatalytic reactor and magnetic separation process that overcomes the difficulty in recovering the used TiO_2 particles. Recently, several studies attempted to prepare the photocatalysts with regard to the photoactive and magnetic properties [16–18]. However, the direct coating of TiO_2 on the magnetite core would decrease the photocatalytic activity because the generated electrons and holes in TiO_2 particles were transferred to the neighboring magnetite rather than to the TiO_2 surface [19]. Xu et al. [20,21] proposed a novel process to synthesize the TiO_2-coated $SiO_2/NiFe_2O_4$ nanosphere as the magnetically separable photocatalyst. The $TiO_2/SiO_2/NiFe_2O_4$ photocatalysts show high stability and photoactivity for the degradation of methyl orange in the solution. The insulating silica layer was adopted to avoid the interactions between the magnetite core and titania coating [16,18–21]. For our best knowledge, there were only few studies about the magnetic TiO_2 polymer composites. Comparing to the TiO_2 photocatalysts with the composition of silica-coated magnetite, the synthesized TiO_2/mPMMA microspheres have the advantages of good insulation property, simple titania-coating process, low density, polymer characteristics, and particle size controllability [15].

In this study, the morphology, BET-specific surface area, magnetic properties, and durability of the TiO_2/mPMMA microspheres have also been characterized. The photocatalytic experiments of PPD are performed in the completely stirred tank reactor under the conditions of various TiO_2/mPMMA microsphere dosages (W_{cat}), initial PPD concentrations (C_{BLb0}), and illumination radiation. The concentration variations of PPD and chemical oxygen demand (COD) of the solution are analyzed at the specified time intervals to study the photocatalytic degradation of PPD. The COD value, which represents a lump of organic compounds in a certain oxidation state, is often used to indicate the treatment efficiency [22]. When some chemical species are oxidized during the photocatalytic process, the decrease in COD is employed to characterize the change of these fractions. Moreover, the photocatalytic kinetics for the PPD and COD reductions associated with the operation parameters have been obtained. In addition, the durability of the TiO_2/mPMMA microspheres in the photocatalytic process is demonstrated by the multi-run experiments.

2. Materials and methods

2.1. Chemicals

PPD, with a chemical formula of $C_6H_8N_2$ purchased from Sigma–Aldrich (St. Louis, MO, USA), has a molecular weight of 108.1, melting point of 143–145 °C, boiling point of 267 °C, and CAS registry number of 106-50-3. The vapor pressure and log octanol/water partition coefficient ($\log K_{ow}$) of PPD are 2.40×10^{-5} atm and 1.53 at 25 °C, respectively [23]. The molecular structure of PPD is shown in Fig. 1. The experimental solutions of different C_{BLb0} were prepared

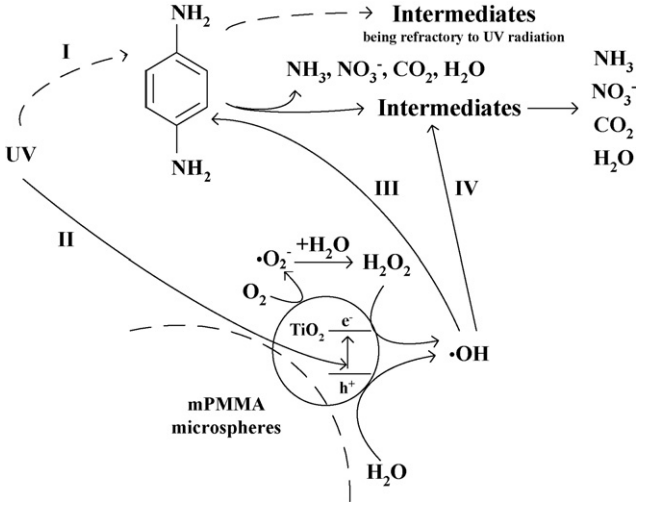

Fig. 1. Molecular structure and simplified photocatalytic scheme of PPD under illumination of UV radiation with TiO_2/mPMMA microspheres.

with deionized water, and the initial pH value of the solution was about 7.04.

Ferric chloride hexahydrate ($FeCl_3 \cdot 6H_2O$, 99%), ferrous chloride tetrahydrate ($FeCl_2 \cdot 4H_2O$, 99%), ammonium hydroxide (NH_4OH, 25%), and methyl methacrylate (MMA) in the reagent grade were purchased from Merck (Darmstadt, Germany). Oleic acid was obtained from Nacalai Tesque (Kyoto, Japan). Polyvinyl alcohol (PVA) was used as a stabilizer and has a molecular weight of 22,000 g/mol as purchased from Acros (Geel, Belgium). Methylene blue trihydrate was purchased from MP Biomedicals (Irvine, CA, USA). Divinylbenzene (DVB) used as the crosslinker was purchased from Tokyo Chemical Industry (Tokyo, Japan). Benzoyl peroxide (BPO) used as an initiator for the polymerization was obtained from Fluka (St. Gallen, Switzerland). Hexane used as the solvent was purchased from Hayashi Pure Chemical Industries (Osaka, Japan). MMA and DVB were purified by the vacuum distillation prior to use. Other chemicals were used without any further purification. Degussa P25 TiO_2 (Dusseldorf, Germany) with the primary particle size and specific surface area of 21 nm and 50 m^2/g, respectively, was employed.

2.2. Preparation of TiO_2/mPMMA microspheres

The co-precipitation method was carried out for the preparation of nano-sized oleic acid-coated magnetite (Fe_3O_4) nanoparticles (OMP). 23.5 g $FeCl_3 \cdot 6H_2O$ and 8.6 g $FeCl_2 \cdot 4H_2O$ were dissolved in 500 mL deionized water under the condition of continuous nitrogen purge. The temperature of the solution was set at 85 °C and then 27.8 mL NH_4OH was added rapidly. Oleic acid was subsequently dropped into the solution within 10 min. The stirring speed was controlled at 600 rpm until a block-like magnetite gel appeared. At that moment, the bulk solution apparently became clear because of the formation of large gel pieces as the aggregation of OMP. The obtained gel was cooled to room temperature and washed several times with deionized water. The shape of the OMP was close to a sphere with a particle diameter of about 8 nm [15].

The mPMMA microspheres were prepared by the modified suspension polymerization. The characteristic of the modified suspension polymerization is to introduce the OMP into the suspension polymerization system for the product of the magnetite-encapsulated polymer particles [15,24,25]. 2 g BPO, 95 mL MMA, 10 mL DVB, and 30 mL hexane along with 15 g magnetite gel were mixed to form the organic phase, which was strongly agitated and subjected to ultrasonication for 3 min to assure the homogeneous dispersion of the OMP. The water phase consisted of 25 g PVA, 5 mL methylene blue trihydrate, and 1000 mL deionized water. Afterwards the two phases were mixed at a stirring speed of 600 rpm in the reactor equipped with four vertical baffles under continuous nitrogen purge. The temperature of the synthetic solution was increased from 45 °C to 55 °C within 1 h, then maintained at 60 °C for 2 h, and finally held at 70 and 80 °C for 1 h each. After the synthesis process was completed, the mPMMA microspheres were separated from the solution by a magnet and washed by deionized water and acetone in turn to remove the attached stabilizer and other impurities on the particle surface.

15 g mPMMA microspheres were mixed thoroughly with 45 g TiO_2 in a 500-mL beaker. The mixture was then placed in the high temperature oven at 220 °C, which is close to the glass transition temperature of the mPMMA microspheres, for the adherence of TiO_2 nanoparticles on the softened surface of the mPMMA microspheres. After being in the oven for 2 h, the beaker containing the TiO_2/mPMMA microspheres and excess TiO_2 nanoparticles was taken out and cooled at room temperature. The TiO_2/mPMMA microspheres were washed with deionized water and then separated with a magnet to remove the non-adhered TiO_2 nanoparticles.

2.3. Characterization of TiO_2/mPMMA microspheres

The morphology and elemental composition of the TiO_2/mPMMA microspheres were observed by the scanning electron microscopy (SEM, JEOL, model JEOL-5610, Tokyo, Japan) and energy dispersive spectrometer (EDS, Oxford INCA Energy, Oxfordshire, UK), respectively. In addition, the transmission electron microscopy (TEM, JEOL, model JEOL-2000EX, Tokyo, Japan) was utilized to investigate the morphology of the microtomed TiO_2/mPMMA microspheres. The porosity of the mPMMA microspheres was estimated by the mercury porosimeter (Micromeritics, model Autopore 9520, Norcross, GA, USA). The BET-specific surface areas of the mPMMA and TiO_2/mPMMA microspheres were analyzed with Micrometrics ASAP 2010 (Atlanta, GA, USA). The magnetization curves of the samples were recorded with the superconducting quantum interference device (SQUID, Quantum Design, model MPMS-XL7, San Diego, CA, USA). The magnetization of the TiO_2/mPMMA microspheres is considered with negligible influence on the photocatalysis due to the nonmagnetic properties of both PPD and TiO_2. The zero point charge of the TiO_2/mPMMA microspheres was measured as pH 6.52 by the instrument (Zetasizer nanoZS90, Malvern, Worcestershire, UK).

2.4. Experimental instrumentation

The airtight reactor with 17.2 cm inside diameter was made of Pyrex glass with an effective volume of 5.5 L and equipped with a water jacket to maintain a constant solution temperature at 25 °C in all photocatalytic experiments. The design of the reactor was based on the criteria for the shape factors of a standard six-blade turbine [26]. Two quartz tubes of 3.8 cm outside diameter symmetrically installed inside the reactor were used to house the UV lamps. The low-pressure mercury lamps of the model HNS 20W/U OZ (Osram, Münich, Germany) and model PL-S 9W (Philips, Eindhoven, Netherlands) principally provided UV radiation at 254 and 365 nm, respectively. The radiation intensity [I] was measured by a digital radiometer (Ultra-Violet Products (UVP), Upland, CA, USA) with the radiation sensors of models DIX-254A and DIX-365A.

The concentration of PPD (C_{BLb}) was analyzed using a high-performance liquid chromatography (HPLC) system, with a 250 mm × 4.6 mm column (model ODS-2, GL Sciences Inc., Tokyo, Japan) and a diode array detector (model L-2455, Hitachi, Tokyo, Japan) at 238 nm. The HPLC solvent with a flow rate of 1.0 mL/min had a composition of methanol/water of 50:50. The injection volume of the analytical solution was 40 μL, and the detection limit of C_{BLb} was 0.01 mg/L. The COD concentration (C_{COD}) was measured by the COD analyzer (model PhotoLab S12, Wissenschaftlich-Technische Werkstatten GmbH & Co., KG (WTW), Weilheim, Germany) using the reagent (model C3/25, WTW, Weilheim, Germany) with the measurement range of 15–150 mg/L. The repeatability of the C_{COD} measurement was performed with the relative standard deviation less than 3%. All fittings, tubings, and bottles were made of stainless steel, Teflon, or glass.

2.5. Photocatalytic experiments of PPD with TiO_2/mPMMA microspheres

The experiments were conducted under various conditions of W_{cat}, C_{BLb0}, and UV radiation intensity ([I]) for the photocatalytic degradation of PPD. About 3.705 L of solution (V_L) was used in each experiment, while the total sampling volume was within 5% of the solution. The stirring speed was 800 rpm to ensure the complete

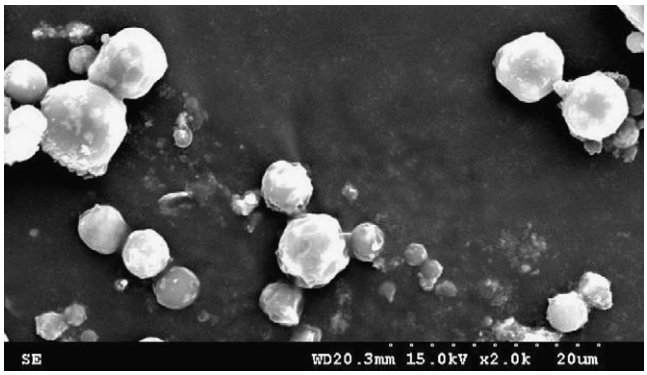

Fig. 2. SEM (2K×) image of TiO_2/mPMMA microspheres.

mixing of the system according to the previous study [27]. Four C_{BLb0} of 3.5, 10, 50, and 332 mg/L were adopted in the experiments. The initial COD concentration (C_{COD0}) is 95.0 mg/L in the case of C_{BLb0} = 50 mg/L, while the C_{COD0} of the solution is proportional to C_{BLb0}. The effect of W_{cat} on the photocatalytic degradation of PPD was evaluated with three different levels of 0.4, 1, and 2.5 g/L.

The contribution of UV radiation was tested with two intensities at 254 nm ($[I_{254}]$) of 0.0889 and 0.174 W/L and one intensity at 365 nm ($[I_{365}]$) of 0.439 W/L. The [I] with the unit of W/L was defined as the average applied power of UV radiation per unit volume in the well-mixed system, which would be proportional to the number of photons absorbed by the solution per unit volume and time. The [I] value was calculated from the product of $[I_{UV}](A_q/V_L)F_s$, where $[I_{UV}]$ is the light intensity measured on the outer surface of

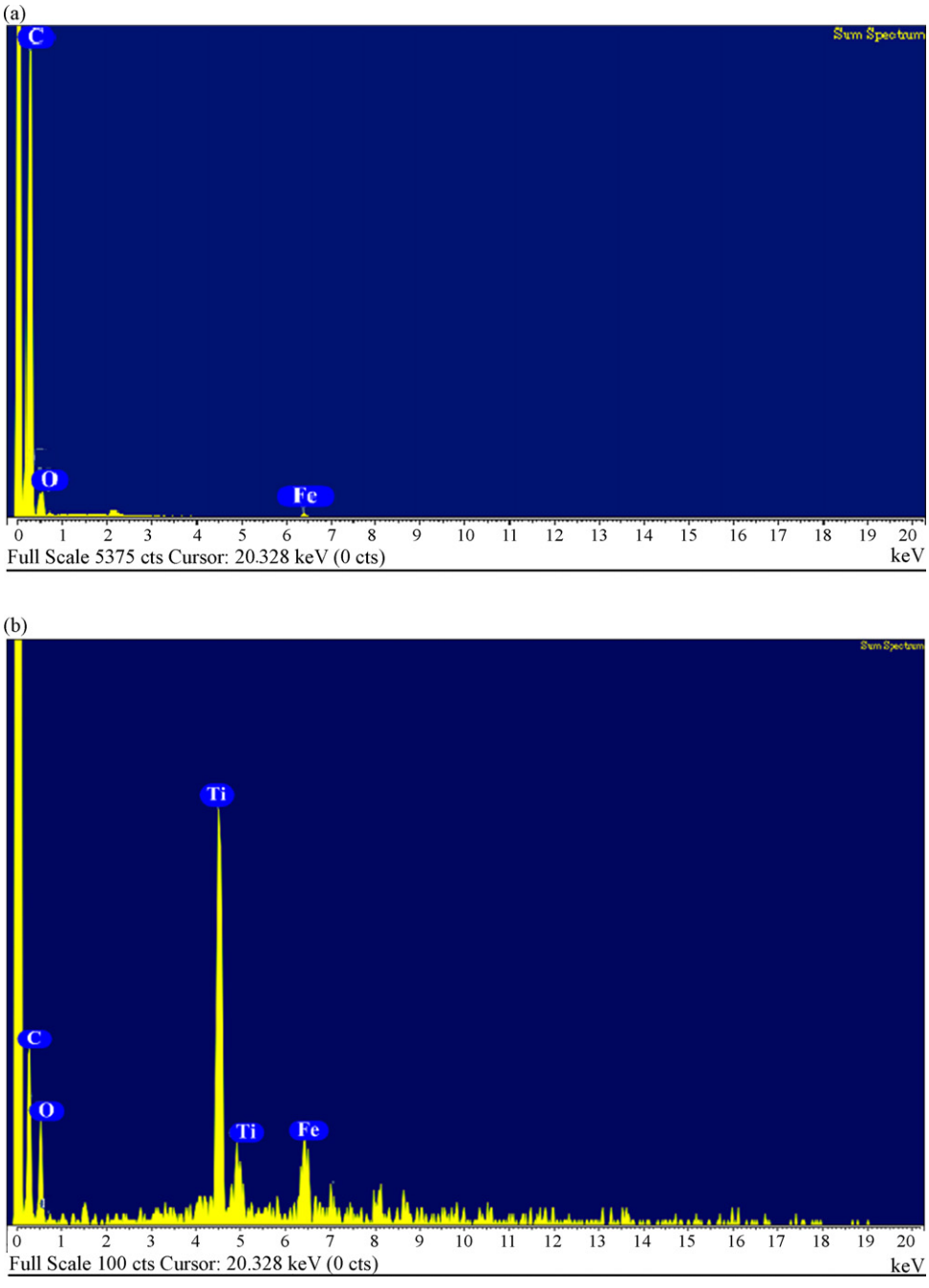

Fig. 3. EDS spectra of mPMMA and TiO_2/mPMMA microspheres. (a) mPMMA and (b) TiO_2/mPMMA.

the quartz tubes by the sensor with the unit of W/cm^2, A_q is the outer area (cm^2) of the quartz tubes submerged in the solution, and F_s is the fraction of the emitting UV light absorbed by the solution [28]. The value of F_s was detected close to the unit in the experiments by measuring the transmittance of the UV radiation through the solution. It should be addressed that the F_s value may relate to the W_{cat} and need to be practically measured in the pilot scale experiments.

The solution with the preset C_{BLb0} and W_{cat} was prepared for the experiments. Before the experiments were started, the UV lamps were set on and cut off by aluminum foil for 30 min to ensure the stability of the UV intensity and solution temperature. Then the UV radiation was introduced into the reactor to begin the photocatalytic degradation of PPD when the system was ready to start. Samples were drawn out from the reactor at desired time intervals in the course of the experiments. The TiO_2/mPMMA microspheres in the samples were immediately recovered by a magnet, and the C_{BLb} and C_{COD} values of the samples were analyzed. Moreover, the multi-run experiments were carried out for five successive runs to test the durability of the TiO_2/mPMMA microspheres.

3. Results and discussion

3.1. Characteristics of TiO_2/mPMMA microspheres

The morphology, BET-specific surface area, EDS, and magnetic properties of the TiO_2/mPMMA microspheres are characterized. The morphology of the TiO_2/mPMMA microspheres is shown by the SEM image in Fig. 2. Furthermore, the mPMMA microspheres are observed with the nonporous structure and BET-specific surface area of 0.776 m^2/g. After the coating of TiO_2 nanoparticles on the mPMMA microspheres, the TiO_2/mPMMA microspheres have a roughly spherical shape, particle size on the order of several micrometers (about 4–8 μm), and higher BET-specific surface area of 2.21 m^2/g. The increase in the BET specific surface area is attributed to the coated TiO_2 nanoparticles on the surface of the mPMMA microspheres. As for the micro-sized TiO_2/mPMMA photocatalysts, the recovery efficiency of such small particles can be significantly enhanced with the application of the magnetic separation compared to the gravity separation [15,24].

The EDS spectra of the mPMMA and TiO_2/mPMMA microspheres are exhibited in Fig. 3. Apparently, the elemental peak of titanium being invisible for the mPMMA microspheres (Fig. 3(a)) would appear after the coating of TiO_2 nanoparticles as indicated in Fig. 3(b). For the further investigation, the distribution patterns of the magnetite and TiO_2 nanoparticles are depicted by the TEM image of the microtomed TiO_2/mPMMA microsphere in Fig. 4. It can be observed that the dispersion of the magnetite nanoparticles encapsulated inside the mPMMA microspheres is considerably uniform. Additionally, the TiO_2 nanoparticles coated on the surface of the mPMMA microspheres form a multilayer coating with the thickness of about 100–250 nm.

The magnetic properties of the mPMMA and TiO_2/mPMMA microspheres are characterized by a SQUID magnetometer at the room temperature as shown in Fig. 5. The magnetization of the samples would approach the saturation values when the applied magnetic field increases to 15,000 Oe. All the magnetization curves show the typical superparamagnetic behavior without the hysteresis loop. Furthermore, the values of the saturation magnetization (Ms), residual magnetization (Mr) per gram, remanence/saturation magnetization ratio (Mr/Ms), and coercivity (Hc) of the samples are listed in Table 1. The mPMMA microspheres have the greater Ms value of 5.92 emu/g. The Ms of the synthesized TiO_2/mPMMA microspheres would decrease to 4.81 emu/g due to the coating of the nonmagnetic TiO_2 nanoparticles. The superparamagnetic properties of the mPMMA and TiO_2/mPMMA microspheres are also reflected in the small Mr/Ms and Hc values. One may notice that the Ms of the synthesized TiO_2/mPMMA microspheres is on the same order as those of the magnetic polymer carriers in the previous studies [25,29,30]. Therefore, the TiO_2/mPMMA microspheres obtained in this work are applicable to the magnetic separation process.

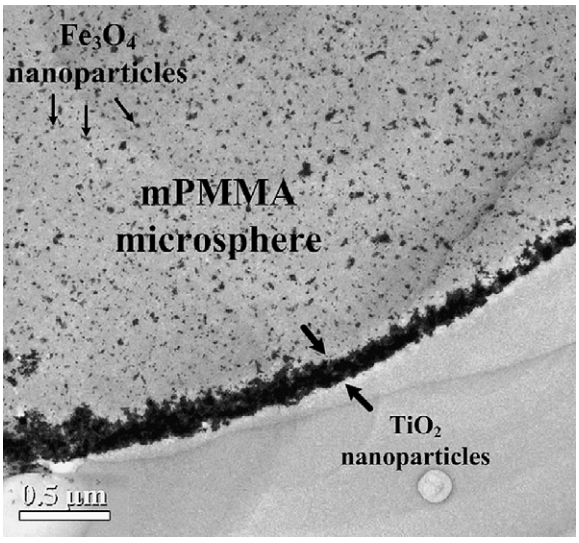

Fig. 4. TEM (6K×) image of microtomed TiO_2/mPMMA microspheres.

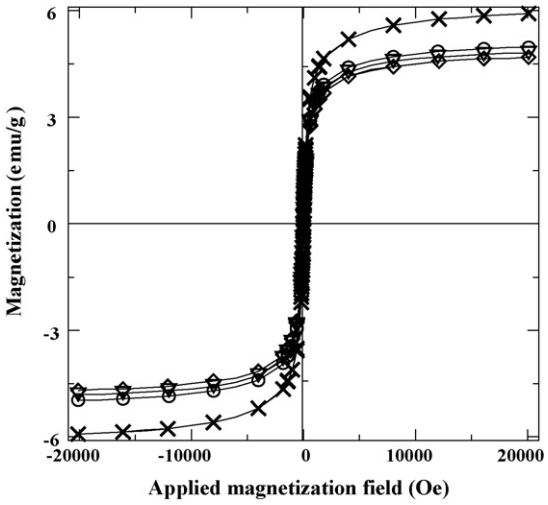

Fig. 5. Magnetization curves of mPMMA and TiO_2/mPMMA microspheres measured by SQUID. (×) mPMMA (obtained from Chen et al. [15]); (▽), (◯), and (◊): new TiO_2/mPMMA, TiO_2/mPMMA used for once, and TiO_2/mPMMA used for five runs, respectively.

Table 1
Magnetic properties of mPMMA and TiO_2/mPMMA microspheres

Samples	Ms (emu/g)	Mr (emu/g)	Mr/Ms	Hc (Oe)
mPMMA[a]	5.92	0.253	0.0427	12.7
New TiO_2/mPMMA	4.81	0.202	0.0421	13.1
TiO_2/mPMMA used for once	4.96	0.204	0.0411	12.7
TiO_2/mPMMA used for five runs	4.69	0.186	0.0397	14.3

[a] Obtained from Chen et al. [15].

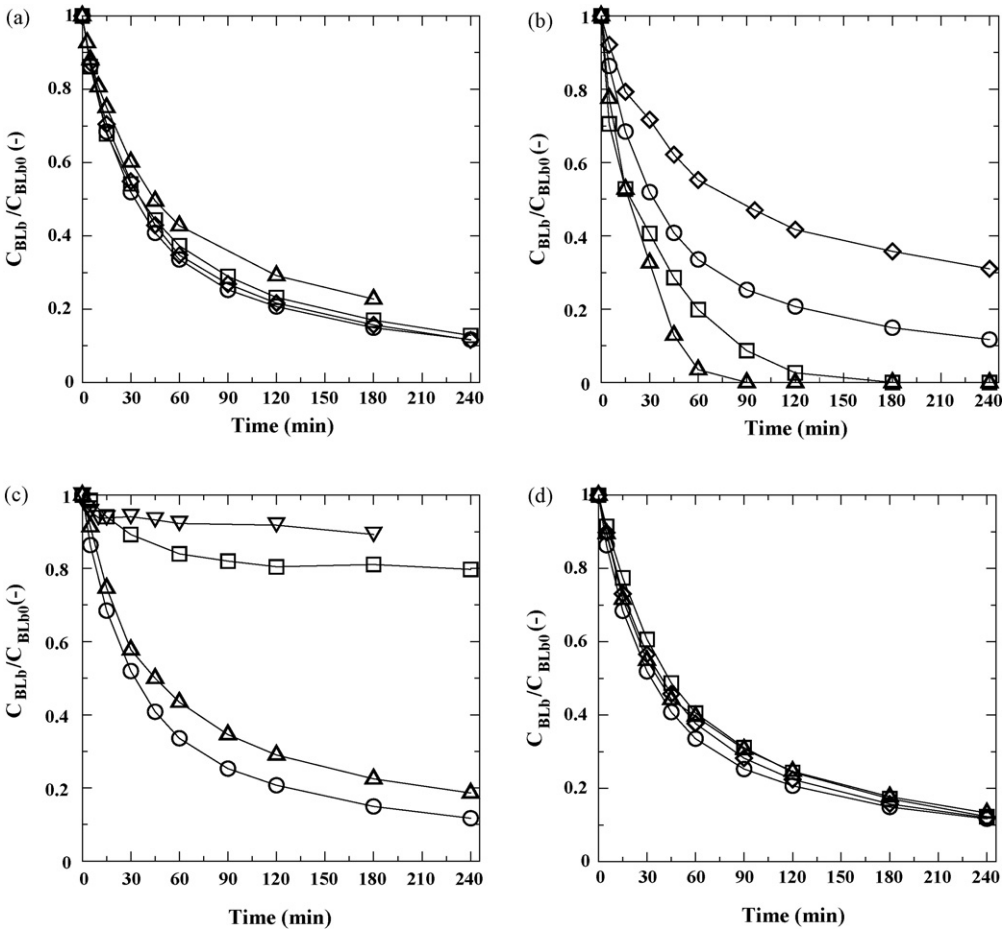

Fig. 6. Variations of C_{BLb}/C_{BLb0} with time for the photocatalytic degradation of PPD with TiO_2/mPMMA microspheres under various experimental conditions. (a) (△), (□), (○), and (◊): W_{cat} = 0, 0.4, 1, and 2.5 g/L; C_{BLb0} = 50 mg/L; $[I_{254}]$ = 0.174 W/L. (b) (△), (□), (○), and (◊): C_{BLb0} = 3.5, 10, 50, and 332 mg/L; W_{cat} = 1 g/L, $[I_{254}]$ = 0.174 W/L. (c) (○) $[I_{254}]$ = 0.174 W/L; (△): $[I_{254}]$ = 0.0889 W/L; (□): $[I_{365}]$ = 0.439 W/L; (▽): $[I]$ = 0 W/L. C_{BLb0} = 50 mg/L, W_{cat} = 1 g/L. (d) (○), (△), (□), and (◊): 1st, 3rd, 4th, and 5th run. C_{BLb0} = 50 mg/L, W_{cat} = 1 g/L, $[I_{254}]$ = 0.174 W/L.

3.2. Photocatalytic degradation and kinetics of PPD

Fig. 6(a–c) show the time variations of C_{BLb}/C_{BLb0} under the experimental conditions of various W_{cat}, C_{BLb0}, and $[I]$, respectively. In Fig. 6(a), the elimination of PPD via the direct photolysis (W_{cat} = 0) with $[I_{254}]$ = 0.174 W/L is found remarkable. This is because the benzene ring containing the amino substitution has a great molar adsorption coefficient of UV radiation [31]. By comparison, the photocatalytic degradation of PPD in the presence of the TiO_2/mPMMA microspheres would have a higher decomposition rate. However, one should note that the mechanisms of the direct photolysis and TiO_2 photocatalysis of PPD are different that is demonstrated by the distinct variations of COD as described in Section 3.3. Furthermore, the effect of W_{cat} on the decomposition rate of PPD is insignificant, indicating that the W_{cat} values employed in this study are sufficient for the utilization of UV radiation.

On the other hand, the effect of C_{BLb0} on the photocatalytic degradation of PPD is remarkable as shown in Fig. 6(b). Although the elimination rate at higher C_{BLb0} seems to be slower in terms of C_{BLb}/C_{BLb0}, the actual removal rate of PPD (dC_{BLb}/dt, mg/(L min)) is evidently higher. The Langmuir–Hinshelwood model is often applied to quantify the photocatalytic reaction rate [32–35]. The initial photocatalytic reaction rate (r_0) is supposed to relate to the initial fraction of TiO_2 surface covered by PPD (θ_B). Further, the equation for the r_0 can be derived as Eq. (1) by combining with Langmuir's isotherm.

$$r_0 = \left.\frac{-dC_{BLb}}{dt}\right|_{t=0} = k_B\theta_B = \frac{k_B K_B C_{BLb0}}{1 + K_B C_{BLb0}} \quad (1)$$

where k_B and K_B are the photocatalytic reaction rate constant and equilibrium adsorption constant of Langmuir's isotherm, respectively.

Moreover, the illumination condition of the UV radiation plays an important role in the photocatalytic degradation of PPD as depicted in Fig. 6(c). The cases with $[I]$ = 0 and $[I_{365}]$ = 0.439 W/L have small removal efficiencies of about 11% and 19% in 180 min, respectively. One may notice that the photocatalytic properties of the TiO_2/mPMMA microspheres are similar to those of the original Degussa P25 TiO_2 particles. The inefficient photoactivity of Degussa P25 TiO_2 particles under UVA illumination at 365 nm has also been found in the previous study [36]. Oppositely, the elimination rate of PPD is remarkably enhanced with the presence of UV radiation at 254 nm. Assuming that the k_B is proportional to the $[I_{254}]$ value [37], Eq. (2) can be obtained by substituting $k_B = k_B'[I_{254}]$ into Eq. (1).

$$\frac{[I_{254}]}{r_0} = \frac{1}{(k_B' K_B C_{BLb0})} + \frac{1}{k_B'} \quad (2)$$

Table 2 summaries the r_0 values under various experimental conditions, demonstrating the significant increase of the r_0 with

Table 2
Values of r_0 and k_{COD} for the photocatalytic degradation of PPD with TiO_2/mPMMA microspheres under various experimental conditions

C_{BLb0} (mg/L)	W_{cat} (g/L)	$[I_{254}]$ (W/L)	r_0 (mg/(L min))	k_{COD}[a] (min^{-1})
3.5	1	0.174	0.160	NM[b]
10	1	0.174	0.597	NM[b]
50	0.4	0.174	1.50	0.00286
50	1	0.0889	0.897	0.00255
50	1	0.174	1.58	0.00352
50	2.5	0.174	1.39	0.00422
332	1	0.174	4.58	0.00386

[a] Obtained from experimental data based on Eq. (3).
[b] Not measured.

higher C_{BLb0} and $[I_{254}]$. All the r_0 values in Table 2 are employed to plot the linear correlation of $[I_{254}]/r_0 = 3.620/C_{BLb0} + 0.0243$ as shown in Fig. 7. The values of k_B' and K_B are determined as 41.2 mg/(W min) and 0.00671 L/mg, respectively. The Langmuir–Hinshelwood model associated with the obtained k_B' and K_B is considered appropriate to describe the photocatalytic elimination of PPD by using the TiO_2/mPMMA microspheres [32,33,37–39]. A simple scheme for the photocatalytic degradation of PPD with the TiO_2/mPMMA microspheres is illustrated in Fig. 1. The photocatalytic mechanism is composed of the generation of the oxidative species such as hydroxyl radicals and the following oxidation of PPD and intermediates. The main products from the photocatalytic degradation of PPD may include nitrate, ammonium, and partially oxidized organics like *p*-dinitrosobenzene and *p*-benzoquinone [40,41]. In addition, the pH value of the suspension during the photocatalytic experiments slightly varies within the range of 6.99–8.03.

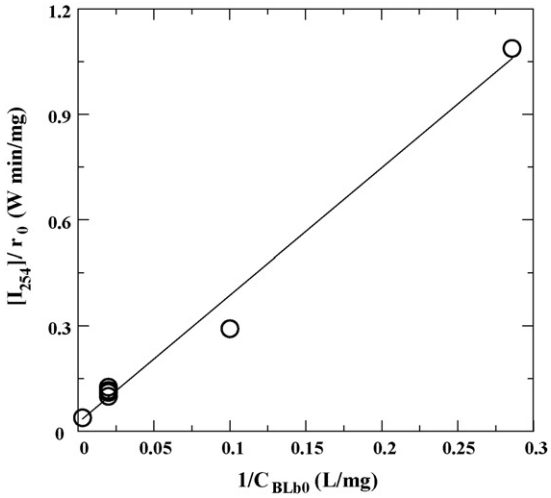

Fig. 7. Linear relationship of $[I_{254}]/r_0$ with $1/C_{BLb0}$ for photocatalytic degradation of PPD with TiO_2/mPMMA microspheres. Correlation: $[I_{254}]/r_0 = 3.620/C_{BLb0} + 0.0243$; $R^2 = 0.986$.

3.3. Reduction of COD in photocatalytic degradation of PPD

To investigate the photocatalytic oxidation of PPD with the TiO_2/mPMMA microspheres, the variations of C_{COD}/C_{COD0} are studied under various experimental conditions. The reduction rate of COD would significantly depend on the W_{cat} as depicted in Fig. 8(a). Note that the direct photolysis of PPD accompanies the negligible

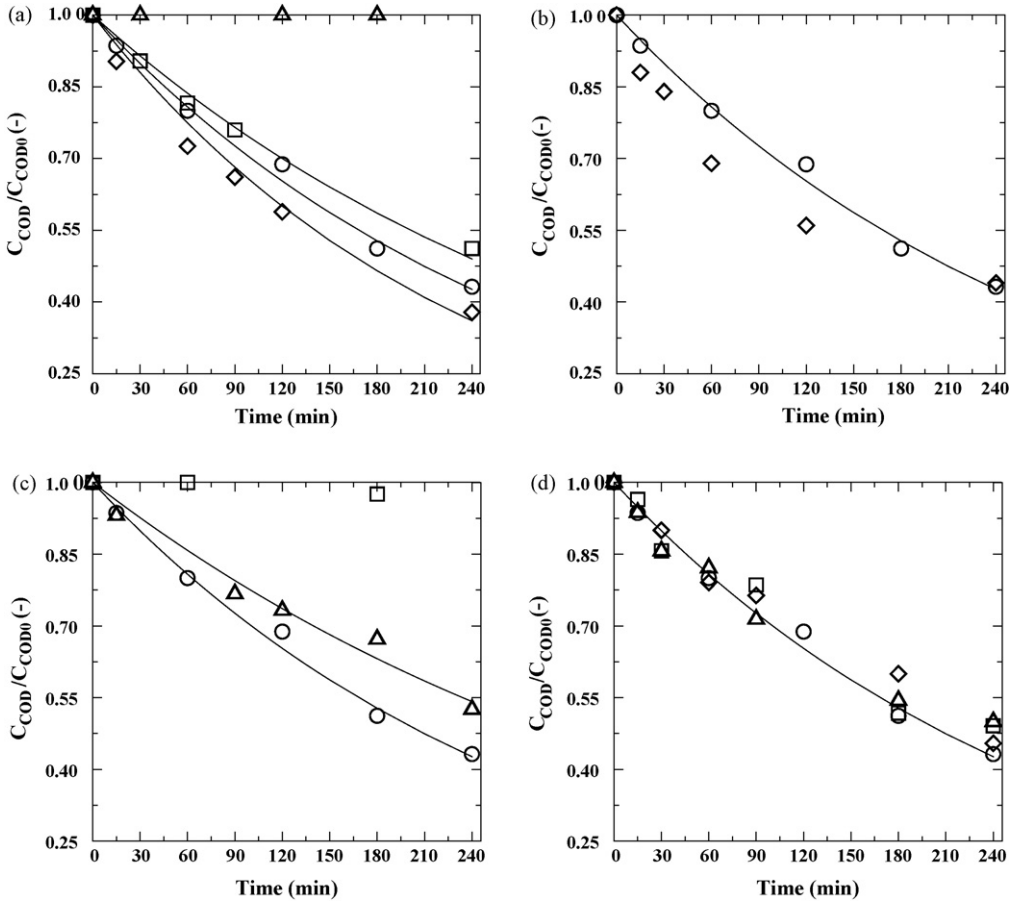

Fig. 8. Variations of C_{COD}/C_{COD0} with time for photocatalytic degradation of PPD with TiO_2/mPMMA microspheres under various conditions of (a) W_{cat}, (b) C_{BLb0}, (c) illumination, and (d) multi-run experiments. Notations and experimental conditions are the same as specified in Fig. 6. Lines: prediction.

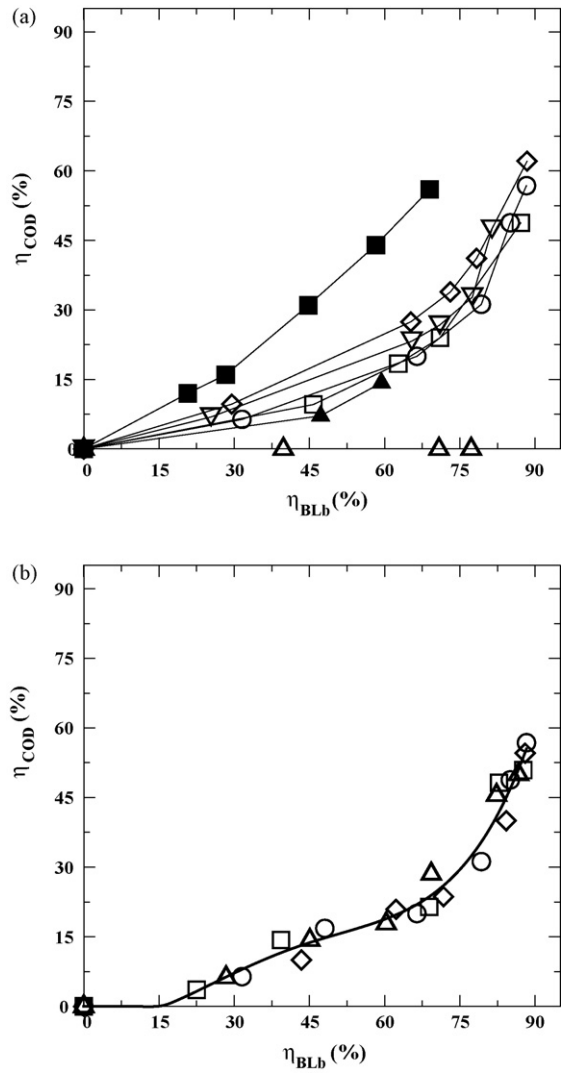

Fig. 9. η_{COD} vs. η_{BLb} for the photocatalytic degradation of PPD with TiO_2/mPMMA microspheres. (a) (▽) C_{BLb0} = 50 mg/L, W_{cat} = 1 g/L, $[I_{254}]$ = 0.0889 W/L. (▲) C_{BLb0} = 10 mg/L, W_{cat} = 1 g/L, $[I_{254}]$ = 0.174 W/L. (■) C_{BLb0} = 332 mg/L, W_{cat} = 1 g/L, $[I_{254}]$ = 0.174 W/L. Other notations and experimental conditions are the same as specified in Fig. 6(a). (b) The multi-run experiments. Notations and experimental conditions are the same as specified in Fig. 6(d). Line: average and smooth curve of experimental data with R^2 = 0.975.

reduction of COD, implying the poor oxidation ability. Evidently, the COD reduction can only be proceeded via the photocatalytic oxidation so that more active sites of the TiO_2/mPMMA microspheres are advantageous to the oxidation reaction. As for different C_{BLb0} in Fig. 8(b), the reduction efficiency of C_{COD}/C_{COD0} is relatively lower in the case of higher C_{BLb0} due to the greater competition of the intermediates for the oxidative species.

Similar to the reduction trend of PPD, the COD elimination is insignificant under the UV illumination of $[I_{365}]$ = 0.439 W/L with the TiO_2/mPMMA microspheres (Fig. 8(c)). The reduction rate of C_{COD}/C_{COD0} remarkably increases with $[I_{254}]$. The pseudo first-order reaction rate equation of Eq. (3) is applied to describe the variation of C_{COD}/C_{COD0} where k_{COD} is the photocatalytic oxidation rate constant [42].

$$\ln\left(\frac{C_{COD}}{C_{COD0}}\right) = -k_{COD}t \quad (3)$$

The values of k_{COD} in Table 2 are regressed from the experimental data of COD reduction. Further, the correlation of k_{COD} associated with W_{cat} and $[I_{254}]$ is obtained as the following equation:

$$k_{COD}\,(\mathrm{min}^{-1}) = 0.00842[I_{254}]^{0.494}W_{cat}^{0.196} \quad (4)$$

As shown in Fig. 8, the prediction of C_{COD}/C_{COD0} based on Eqs. (3) and (4) reveals good agreement with the experimental data.

The relationship between the reduction percentages of COD (η_{COD}) and PPD (η_{BLb}) during the photocatalytic degradation of PPD is illustrated in Fig. 9(a). For $\eta_{BLb} \leq 30\%$, the increase in η_{COD} is small due to the fact that the initial intermediates generated from the decomposition of PPD still contribute large amount of COD. While η_{BLb} is greater than 30%, η_{COD} starts to noticeably increase with η_{BLb}. It is obvious that the variation of η_{COD} with η_{BLb} mainly depends on the θ_B value ($=K_BC_{BLb0}/(1+K_BC_{BLb0})$). The ratio of η_{COD} to η_{BLb} would be higher in the case of higher θ_B at the same η_{BLb}. For example, the η_{COD}/η_{BLb} ratio is about 0.765, 0.335, 0.238, and 0 for the cases of θ_B = 0.69, 0.251, 0.063, and 0, respectively, when η_{BLb} is 60%. The reason for this phenomenon is that the contribution of the photocatalysis to the η_{BLb} would increase with higher θ_B, thus accompanying the greater η_{COD}. In the later photocatalytic stage ($\eta_{BLb} > 75\%$), η_{COD} starts to increase with η_{BLb} remarkably because more oxidative species are consumed for the oxidation of the intermediates. Therefore, the η_{BLb} value at the specific θ_B can be used as the supplementary index of the η_{COD} for the photocatalytic degradation of PPD.

The durability of the TiO_2/mPMMA microspheres is demonstrated by the slight variations of the appearance observation, thermogravimetric analysis, magnetization properties, and photoactivity after the multi-run experiments. Figs. 5, 6(d) and 8(d) show the satisfactory stability of the magnetic characteristics and photocatalytic performance for the TiO_2/mPMMA microspheres in the repetitive cycles of PPD degradation. The reliability of the relationship between η_{COD} and η_{BLb} has also been confirmed by the repetition as depicted in Fig. 9(b). The good durability of the TiO_2/mPMMA microspheres is due to that the crosslinked polymer usually presents the adequate resistance to the TiO_2 photocatalysis [43]. Furthermore, the photo-induced reaction mainly happens on the multilayer surface of the TiO_2 coating resulting in indirect contact to the mPMMA matrix. Although the TiO_2/mPMMA microspheres may lose some TiO_2 coating from the long-term use, it is possible to restore the used TiO_2/mPMMA microspheres by repeating the titania-coating process for the recovery of the photoactivity.

4. Conclusions

The novel titanium dioxide-coated magnetic poly(methyl methacrylate) (TiO_2/mPMMA) microspheres are synthesized and employed for the photocatalytic degradation of *p*-phenylenediamine (PPD). The TiO_2/mPMMA microspheres have the particle size of several micrometers, BET-specific surface area of 2.21 m^2/g, coated TiO_2 layer with the thickness of about 100–250 nm, and saturation magnetization of 4.81 emu/g. The photocatalytic decomposition of PPD significantly increases with the initial PPD concentration (C_{BLb0}, mg/L) and UV radiation intensity at 254 nm ($[I_{254}]$, W/L), while slightly varies with the TiO_2/mPMMA microsphere dosage (W_{cat}, g/L). The initial photocatalytic reaction rate of PPD is obtained as $-dC_{BLb}/dt = k_BK_BC_{BLb0}/(1+K_BC_{BLb0})$ with the photocatalytic reaction rate constant (k_B) and equilibrium adsorption constant of Langmuir's isotherm (K_B) of $41.2[I_{254}]$ mg/(L min) and 0.00671 L/mg, respectively. The reduction rate of chemical oxidation demand (COD) in the photocatalytic degradation of PPD follows the pseudo-first-order reaction rate equation with the photocatalytic oxidation rate constant (k_{COD}, min^{-1}) as $0.00842[I_{254}]^{0.494}W_{cat}^{0.196}$. The clear-cut relationship between the reduction percentages of COD and PPD for the photo-

catalytic degradation of PPD has been presented. In addition, the good durability of the TiO_2/mPMMA microspheres is demonstrated by the stability of the magnetization properties and photocatalytic performance in the multi-run experiments. Consequently, this study can provide the useful information about the characteristics of the TiO_2/mPMMA microspheres and their application to the photocatalytic degradation of PPD in an aqueous solution.

Acknowledgment

This study was supported by the National Science Council of Taiwan under Grant NSC 94-2218-E-151-014.

References

[1] B.N. Ames, H.O. Kammen, A.E. Yamasaki, Hair dyes are mutagenic: identification of a variety of mutagenic ingredients, Proc. Natl. Acad. Sci. U.S.A. 72 (1975) 2423–2427.
[2] R. Wilson, Risks posed by various components of hair dyes, Arch. Dermatol. Res. 278 (1985) 165–170.
[3] C.M. Burnett, Multigeneration reproduction and carcinogenicity studies in Sprague–Dawley rats exposed topically to oxidative hair-colouring formulations containing *p*-phenylenediamine and other aromatic amines, Food Chem. Toxicol. 26 (1988) 467–474.
[4] P. Tachon, J. Cotovio, K.G. Dossou, M. Prunieras, Alternative method for checking toxicity of hair dyes, Int. J. Cosmet. Sci. 8 (1986) 265–273.
[5] Y. Kawakubo, B. Blömeke, H. Merk, *p*-Phenylenediamine (PPD) *N*-acetylation in human skin cytosol, J. Invest. Dermatol. 110 (1998) 533.
[6] M.R. Hoffmann, S.T. Martin, W. Choi, D.W. Bahnemann, Environmental applications of semiconductor photocatalysis, Chem. Rev. 95 (1995) 69–96.
[7] Ø. Olsvik, T. Popovic, E. Skjerve, K.S. Cudjoe, E. Hornes, Magnetic separation techniques in diagnostic microbiology, Clin. Microbiol. Rev. 7 (1994) 43–54.
[8] K. Landfester, L.P. Ramírez, Encapsulated magnetite particles for biomedical application, J. Phys. Condens. Mat. 15 (2003) 1345–1362.
[9] P. Kronick, R.W. Gilpin, J. Biochem, Use of superparamagnetic particles for isolation of cells, J. Biochem. Biophys. Methods 12 (1986) 73–80.
[10] X.H. Li, Z.G. Sun, Synthesis of magnetic polymer microspheres and application for immobilization of proteinase of *Balillus sublitis*, J. Appl. Polym. Sci. 58 (1995) 1991–1997.
[11] T. Abudiab, R.R. Beitle, Preparation of magnetic immobilized metal affinity separation media and its use in the isolation of proteins, J. Chromatogr. A 795 (1998) 211–217.
[12] D.K. Kim, Y. Zhang, W. Voit, K.V. Kao, J. Kehr, B. Bjelke, M. Muhammed, Superparamagnetic iron oxide nanoparticles for bio-medical applications, Scripta Mater. 44 (2001) 1713–1717.
[13] E.B. Denkbaş, E. Kiliçay, C. Birlikseven, E. Öztürk, Magnetic chitosan microspheres: preparation and characterization, React. Funct. Polym. 50 (2002) 225–232.
[14] T. Dahlke, Y.H. Chen, M. Franzreb, W.H. Höll, Continuous removal of copper ions from dilute feed streams using magnetic weak-base anion exchangers in a continuous stirred tank reactor (CSTR), React. Funct. Polym. 66 (2006) 1062–1072.
[15] Y.H. Chen, Y.Y. Liu, R.H. Lin, F.S. Yen, Characterization of magnetic poly(methyl methacrylate) microspheres prepared by the modified suspension polymerization, J. Appl. Polym. Sci. 108 (2008) 583–590.
[16] S. Watson, D. Beydoun, R. Amal, Synthesis of a novel magnetic photocatalyst by direct deposition of nanosized TiO_2 crystals onto a magnetic core, J. Photochem. Photobiol. A 148 (2002) 303–313.
[17] S. Rana, R.S. Srivastava, M.M. Sorensson, R.D.K. Misra, Synthesis and characterization of nanoparticles with magnetic core and photocatalytic shell: anatase TiO_2–$NiFe_2O_4$ system, Mater. Sci. Eng. 119 (2005) 144–151.
[18] W. Fu, H. Yang, L. Chang, H. Bala, M. Li, G. Zou, Anatase TiO_2 nanolayer coating on strontium ferrite nanoparticles for magnetic photocatalyst, Colloid Surf. A 289 (2006) 47–52.
[19] S. Tawkaew, S. Supothina, Preparation of agglomerated particles of TiO_2 and silica-coated magnetic particle, Mater. Chem. Phys. 108 (2008) 147–153.
[20] S. Xu, W. Shangguan, J. Yuan, M. Chen, J. Shi, Preparations and photocatalytic properties of magnetically separable nitrogen-doped TiO_2 supported on nickel ferrite, Appl. Catal. B: Environ. 71 (2007) 177–184.
[21] S. Xu, W. Shangguan, J. Yuan, M. Chen, J. Shi, Z. Jiang, Synthesis and performance of novel magnetically separable nanospheres of titanium dioxide photocatalyst with egg-like structure, Nanotechnology 19 (2008) 095606.
[22] I.A. Balcıoğlu, M. Ötker, Treatment of pharmaceutical wastewater containing antibiotics by O_3 and O_3/H_2O_2 processes, Chemosphere 50 (2003) 85–95.
[23] R.P. Schwarzenbach, P.M. Gschwend, D.M. Imboden, Environmental Organic Chemistry, 1st ed., John Wiley & Sons, New York, New York, 1993.
[24] Z.Y. Ma, Y.P. Guan, X.Q. Liu, H.Z. Liu, Preparation and characterization of micron-sized non-porous magnetic polymer microspheres with immobilized metal affinity ligands by modified suspension polymerization, J. Appl. Polym. Sci. 96 (2005) 2174–2180.
[25] Z.Y. Ma, Y.P. Guan, X.Q. Liu, H.Z. Liu, Covalent immobilization of albumin on micron-sized magnetic poly(methyl methacrylate-divinylbenzene-glycidyl methacrylate) microspheres prepared by modified suspension polymerization, Polym. Adv. Technol. 16 (2005) 554–558.
[26] W.L. McCabe, J.C. Smith, P. Harriott, Unit Operations of Chemical Engineering, 5th ed., McGraw-Hill, New York, NY, 1993.
[27] Y.H. Chen, C.Y. Chang, S.F. Huang, N.C. Shang, C.Y. Chiu, Y.H. Yu, P.C. Chiang, J.L. Shie, C.S. Chiou, Decomposition of 2-naphthalenesulfonate in electroplating solution by ozonation with UV radiation, J. Hazard. Mater. 118 (2005) 177–183.
[28] Y.H. Chen, C.Y. Chang, C.C. Chen, C.Y. Chiu, Kinetics of ozonation of 2-mercaptothiazoline in an electroplating solution combined with UV radiation, Ind. Eng. Chem. Res. 45 (2006) 4936–4943.
[29] Y. Lee, J. Rho, B. Jung, Preparation of magnetic ion-exchange resins by the suspension polymerization of styrene with magnetite, J. Appl. Polym. Sci. 89 (2003) 2058–2067.
[30] Z.Y. Ma, Y.P. Guan, H.Z. Liu, Affinity adsorption of albumin on cibacron blue F3GA-coupled non-porous micrometer-sized magnetic polymer microspheres, React. Funct. Polym. 66 (2006) 618–624.
[31] P. Mazellier, A. Rachel, V. Mambo, Kinetics of benzenesulfonates elimination by UV and UV/H_2O_2, J. Photochem. Photobiol. A 163 (2004) 389–393.
[32] W. Leng, H. Liu, S. Cheng, J. Zhang, C. Cao, Kinetics of photocatalytic degradation of aniline in water over TiO_2 supported on porous nickel, J. Photochem. Photobiol. A 131 (2000) 125–132.
[33] E. Evgenidou, K. Fytianos, I. Poulios, Photocatalytic oxidation of dimethoate in aqueous solutions, J. Photochem. Photobiol. A 175 (2005) 29–38.
[34] J.P.S. Valente, P.M. Padilha, A.O. Florentino, Studies on the adsorption and kinetics of photodegradation of a model compound for heterogeneous photocatalysis onto TiO_2, Chemosphere 64 (2006) 1128–1133.
[35] S. Kaur, V. Singh, TiO_2 mediated photocatalytic degradation studies of reactive red 198 by UV irradiation, J. Hazard. Mater. 141 (2007) 230–236.
[36] A. Mills, A. Lepre, N. Elliott, S. Bhopal, I.P. Parkin, S.A. O'Neill, Characterisation of the photocatalyst Pilkington ActivTM: a reference film photocatalyst, J. Photochem. Photobiol. A 160 (2003) 213–224.
[37] N. Daneshvar, M. Rabbani, N. Modirshahla, M.A. Behnajady, Kinetic modeling of photocatalytic degradation of acid red 27 in UV/TiO_2 process, J. Photochem. Photobiol. A 168 (2004) 39–45.
[38] M. Hügül, E. Erçag, R. Apak, Kinetic studies on UV-photodegradation of some chlorophenols using TiO_2 catalyst, J. Environ. Sci. Health A37 (2002) 365–383.
[39] M. Muruganandham, M. Swaminathan, TiO_2-UV photocatalytic oxidation of reactive yellow 14: effect of operation parameters, J. Hazard. Mater. 135 (2006) 78–86.
[40] T. Zhang, T.K. Oyama, S. Horikoshi, H. Hidaka, J. Zhao, N. Serpone, Photocatalyzed *N*-demethylation and degradation of methylene blue in titanium dispersions exposed to concentrated sunlight, Sol. Energy Mater. Sol. C 73 (2002) 287–303.
[41] P. Piccinini, C. Minero, M. Vincenti, E. Pelizzetti, Photocatalytic mineralization of nitrogen-containing benzene derivatives, Catal. Today 39 (1997) 187–195.
[42] A.B. Prevot, C. Baiocchi, M.C. Brussino, E. Pramauro, P. Savarino, V. Augugliaro, G. Marcì, L. Palmisano, Photocatalytic degradation of acid blue 80 in aqueous solution containing TiO_2 suspensions, Environ. Sci. Technol. 35 (2001) 971–976.
[43] Q. Tang, J. Lin, Z. Wu, J. Wu, M. Huang, Y. Yang, Preparation and photocatalytic degradability of TiO_2/polyacrylamide composite, Eur. Polym. J. 43 (2007) 2214–2220.